Journal of Corrosion and Materials *J. Corros. Mater.* (2025) 4(2), 159–172.
www.corromat.com

Resolution–Absorption Design Windows for Additively Manufactured Terahertz Quasi-Optical Components

Pier Luigi Luisi[1,*]

[1] *Department of Science, Roma Tre University, Viale Guglielmo Marconi 446, 00146 Rome, Italy*

[*] Corresponding author: luisi@mat.ethz.ch

(Received: 30 July 2025. Received in revised form: 13 October 2025. Accepted: 25 October 2025. Published online: 30 December 2025.)

Abstract

In order for additively manufactured terahertz quasi-optics to meet a necessary condition of combined optics and manufacturing, the operating wavelength determines the permissible scales of features and surfaces, while the material path length defines whether the absorption prevents the transmission. A solution in printing smooth enough geometry will fail due to the loss of resin in case of millimetre-thick lens, and a solution in transparent polymer printing will fail if the scale of features printed is too large compared to the operating wavelength. The calculations presented above establish the required trade-off for material extrusion, material jetting, vat photopolymerization and powder bed fusion using nineteen printable materials, five composite property paths, ten terahertz frequencies and three optical path lengths. Wavelength-normalized feature ratios, wavelength-normalized roughness ratios and Beer-Lambert transmission through 0.5, 1.0 and 2.0 mm paths have been found according to the data presented in the tables. The best absorption-limited transmission belongs to material extrusion in terms of low-loss filaments, which is 0.905 through 1 mm path for $\alpha = 1$ cm^{-1}, while its mean feature size 415.17μm sets its wavelength-based geometry limit at 0.72 THz. Vat photopolymerization ensures the largest possible geometry range, which is 3.72 THz in terms of wavelength-based feature size and 10.56 THz in terms of wavelength-based roughness, however, 1 mm transmission is only 0.150 for the smallest process-level resin absorption coefficient of 19 cm^{-1}. Material jetting provides the largest build-rate value while loosing majority of transmitted intensity in case of millimetre-scale paths. Powder bed fusion is reserved for reflective or structural terahertz components until transmissive dielectric constant values of printed material are determined. In summary, the proposed selection criterion is tailored for the particular component: thick optics around 1 THz must rely on low loss extruded COC, HDPE or PS, while surface-relief and thin phase structures at 2-3 THz require sub-micron resolution with careful management of resin loss and optical path length.

Keywords: terahertz optics; additive manufacturing; optical thickness; material extrusion; vat photopolymerization; surface roughness; absorption coefficient; quasi-optics

1. Introduction

The terahertz frequency regime is located between microwave electronics and infrared photonics and normally spans frequencies from 0.1 to 10 THz. The significance of this range was discussed in the seminal review of its scientific and technological relevance [1]. Terahertz imaging and spectroscopy techniques make use of the sensitivity of this frequency range to molecular and collective excitations [2]. Time-domain imaging confirms its usefulness for non-ionizing inspection and material identification [3]. Modern sources and detectors have extended the applicability of terahertz systems [4]. The wireless applications literature sees this range as an option for very high bandwidth communications [5]. Its deployment requires lenses, waveplates, phase plates, polarizers, waveguides, filters and reflectors preserving the amplitude and phase of the optical field. Quasi-optical engineering established the requirements for optical components in millimetre and sub-millimetre systems [6]. The terahertz spectroscopy reviews explain how optical components affect measured field amplitude and phase [7]. Diffractive optics literature additionally emphasizes the need for precisely formed terahertz phase components [8]. Contrary to visible optics, terahertz quasi-optics cannot count on a well-developed range of low-cost transparent materials and precisely manufactured components. Polymers, ceramics and metallized substrates are frequently used but every combination of material and processing imposes its penalty due to absorption, surface scattering, dispersion, roughness and dimensional error.

Additive manufacturing appears attractive in this case because many terahertz components are made of thick polymer bodies, channels inside them, freeform geometries, lattice supports, integrated mounts or fine surface textures. Three-dimensional printing has been used to manufacture functional terahertz lenses [9]. The dielectric structures produced via 3D printing also allow making diffractive gratings and other beamforming components [10]. Hollow-core terahertz fibres are another example of usefulness of additive manufacturing for internal optical channels [11]. Printed waveplates allow for manipulating polarization using precise anisotropy of the structure [12]. Freeform phase plates represent further development in this direction and are used for precise wavefront control [13]. Additively manufactured waveguide devices demonstrate the potential of combining optical propagation with integrated mechanical alignment [14]. This is particularly true when the function of optical, mechanical and mounting parts is combined in a single component. Metal additive manufacturing can enable reflective and mechanically tough sub-millimetre optics [15]. The 3D printing technique allows reducing the distance from electromagnetic design to the physical component for polymers [16]. Reviews of printed terahertz devices illustrate how process choice defines the range of available geometries of components [17]. The potential of manufacturing does not eliminate the optical challenges. A rough surface can scatter terahertz waves, a pore field in the interior can change the effective refractive index and an absorbing polymer matrix can attenuate the beam before its phase profile is useful.

The challenge is that the governing tolerances depend on frequency. At 1 THz the wavelength in vacuum is about 300 μm, while at 10 THz it is only about 30 μm. Surface roughness less than 15 μm may satisfy the $\lambda/20$ criterion at 1 THz, while the same roughness is way above the 1.5 μm criterion at 10 THz. Similar dependence exists for minimum feature size. Low-loss potential of non-polar filaments made of extruded cyclic olefin copolymer has been demonstrated [18]. Polyethylene optics made using material extrusion is another route for terahertz transmission [19]. Nevertheless, process studies show that roadways, ridges and minimum feature size become significant for sub-millimetre wavelengths [20]. Vat photopolymerization allows to produce smoother surfaces and finer features. Measurements of commercial resins printed in terahertz frequency range reveal considerable absorption of these materials in the terahertz band [21]. Material surveys confirm that absorption of the photopolymer is the major loss mechanism in this range [22]. High throughput and smooth surfaces are among advantages of material jetting but the absorption of the resins becomes a severe problem for thick optical components. Powder bed fusion provides reflective or structural parts useful in terahertz applications [15]. Both polymer and metal powder-based processes, however, require detailed characterization of roughness and optical losses [23].

The selection of a component is considered as a frequency-thickness decision in this work. For a certain terahertz frequency and thickness of the material path the process family is assigned to the physical criterion that governs the use of this process: absorption, feature size, roughness or absence of transmissive optical constants of the printed state. A 0.5 mm phase plate and a 2 mm refractive lens may be made using different processes even if both components are made of the same polymer. A process can be smooth but feature-limited, or low-loss but geometrically coarse. Therefore, frequency and thickness are dealt with as independent parameters and each process is characterized by the criterion that limits the component first.

Spectral diagram in Figure 1 compares the four process families to the terahertz wavelength that is constantly decreasing.

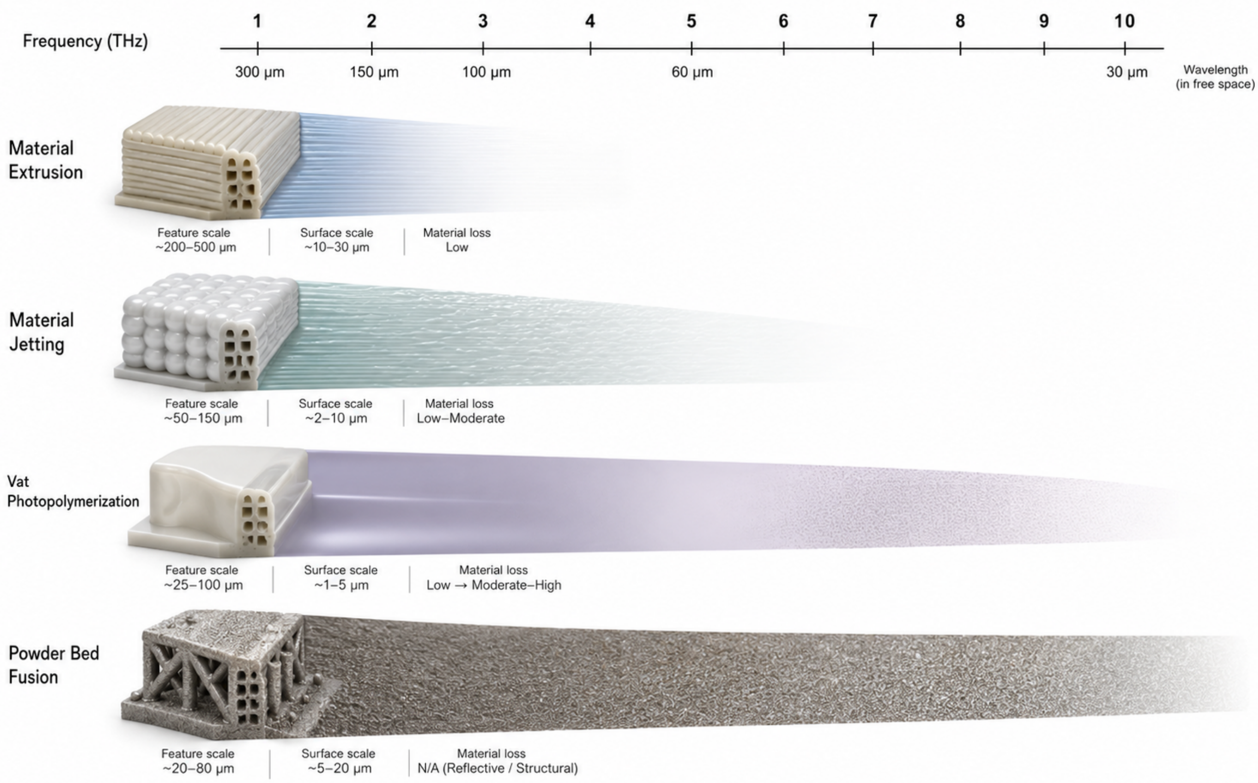

Figure 1: THz frequency, process geometry and material loss.

The contrast illustrated in Figure 1 explains why a universal ranking of the processes is not possible. Material extrusion looks attractive in the low-frequency region because it allows using low-loss polymers but its feature scale and surface texture limit the applicability as the wavelength shortens. Vat photopolymerization maintains visual continuity in a wider region of frequencies because it provides smaller features and smoother surfaces. However, loss layer in the figure highlights the absorption penalty of the resins in this region. Material jetting belongs to the high-throughput but loss-sensitive regime. Powder bed fusion is illustrated as the rougher and more reflective process, which agrees with its greater involvement in metallic and structural terahertz optics.

2. Optical and Manufacturing Background

Design of terahertz optics is constrained by the refractive index of the material, the distance the ray passes and the surface geometry, imposing the necessary phase pattern [24]. Inverse time-domain spectroscopy is a well-established approach to characterize the refractive index and absorption of the polymer [24]. Enhanced inversion algorithms can now provide the optical constants and layer thicknesses simultaneously [25]. Polymer spectroscopy demonstrates that chemical composition strongly affects terahertz absorption [26]. Comparison of the measurements establishes that non-polar polymers generally have less loss compared to polar ones [27]. Molecular dynamics analysis relates this effect to vibrations and dipole moment variations [28]. Modern surveys extend the comparison to printable polymers [29]. It is the reason that COC, HDPE and PS are suitable materials for terahertz optics, while PLA, PVA, nylon and numerous acrylic photopolymers are absorbing at 1 THz.

The optical properties of the materials cannot be evaluated independently from the printed structure. Nozzle diameter and temperature affect the optical parameters of fused filament COC [30]. Raster distance and orientation affect porosity and inter-road bonding [31]. Layer-by-layer structure introduces ridging and anisotropy in the printed optical component [32]. Porosity can lead to lower density and altered absorption but can also cause fluctuations of refractive index and scattering of terahertz radiation. High speed or weakly bonded roads can create empty spaces, and the printed component cannot have optical properties of bulk polymer pellet. Recent studies of COC confirm that the optimization of parameters can affect absorption and refractive index enough to make process selection different [33].

Photopolymer manufacturing occupies the other region of the design space. Stereolithography is capable of producing smaller features and smoother surfaces compared to standard material extrusion [34]. Digital light processing extends this possibility with the projection-based curing layer-by-layer [35]. Material jetting can provide smooth surfaces and multilayering in one process [36]. Resin libraries of these processes are often optimized for curing speed, viscosity, mechanical properties and visual appearance, not for low-absorption terahertz transmission. Acrylates and methacrylates, monomers, initiators and other additives can create additional absorption bands. Ceramic-filled photopolymers can change refractive index but increase processing viscosity [37]. Silica filled resin systems demonstrate the competing influence of fillers load and depth of cure [38]. Studies of terahertz composites demonstrate the impact of similar additions on absorption and phase delay [39]. Thus, photopolymer composites imply trade-off between optical constants and print accuracy.

Surface roughness sets another wavelength dependent limit. Terahertz transmission of roughened PTFE demonstrates that scattering increases when the surface height becomes comparable to the wavelength [40]. Analysis of optical tolerances gives the corresponding limit of surface height for printed components [41]. $\lambda/10$ surface may be sufficient for some optical elements but $\lambda/20$ surface is more desirable for terahertz phase sensitive surfaces. Surface treatment and vapor smoothing can eliminate layer ridges of polymer prints [42]. Mechanical polishing and coating can be applied to metal surfaces but can change curvature and phase relief steps [43]. Thus, the choice of manufacturing technology is determined by optical requirements, not just by the as-printed surface number.

Build speed adds production requirement after passing the optical ones. Material jetting can print several components with rather high build rate, while vat photopolymerization can provide high resolution with lower build speed. Material extrusion can be very fast with high nozzle diameter and deposition rate but it decreases feature fidelity. Two-photon polymerization can print sub-micron structures in high resolution micro-printing [44]. Electrohydrodynamic printing can produce features with tens of microns [45]. Material jetting and direct-write methods can print fine lines in comparison with conventional fused filament fabrication [36]. These approaches demonstrate the ultimate resolution of additive manufacturing, but their build rate, costs, materials selection and component size do not allow them to be used for production of terahertz lenses. Therefore, this paper will consider common manufacturing technologies keeping frequency and thickness logic to compare them.

3. Numerical Inputs and Derived Quantities

The calculations rely on four process entries, nineteen material entries, five composite-property paths, ten operating frequencies and three optical path lengths. Process and material values are taken from the tabulated optical and manufacturing values of Phillips et al. [46]. The numerical setup retains three independent coordinates: operating frequency, path length and material-process combination. Keeping these coordinates gives the ability to consider the same process as applicable for one component category and not for another.

The wavelengths in Table 1 determine the frequency coordinate and are further used in calculating the acceptable roughness scale and comparing the printability feature sizes with the wavelength. In Table 1, the use of both $\lambda/10$ and $\lambda/20$ is kept for transparency, although the further calculation uses the strict limit of $\lambda/20$ for roughness.

Table 1: Wavelength and surface limits.

Frequency (THz)	Wavelength λ (μm)	$\lambda/10$ (μm)	$\lambda/20$ (μm)
1	300	30.0	15.00
2	150	15.0	7.50
3	100	10.0	5.00
4	75	7.5	3.75
5	60	6.0	3.00
6	50	5.0	2.50
7	43	4.3	2.15
8	37	3.7	1.85
9	33	3.3	1.65
10	30	3.0	1.50

Such material-process pairs provide information about the central frequency penalty. A process with 12 μm mean roughness is tolerable in terms of 15 μm $\lambda/20$ limit at 1 THz, but it becomes incompatible with the 5 μm limit at 3 THz. This decrease makes short-wavelength diffractive and phase-relief components significantly harder than low-frequency refractive lenses.

The surface-tolerance corridor in Figure 2 graphically illustrates Table 1 in comparison with the four process means. The surface-tolerance corridor is shown here because it highlights the fact that roughness tolerance is not a constant manufacturing challenge; it collapses depending on frequency.

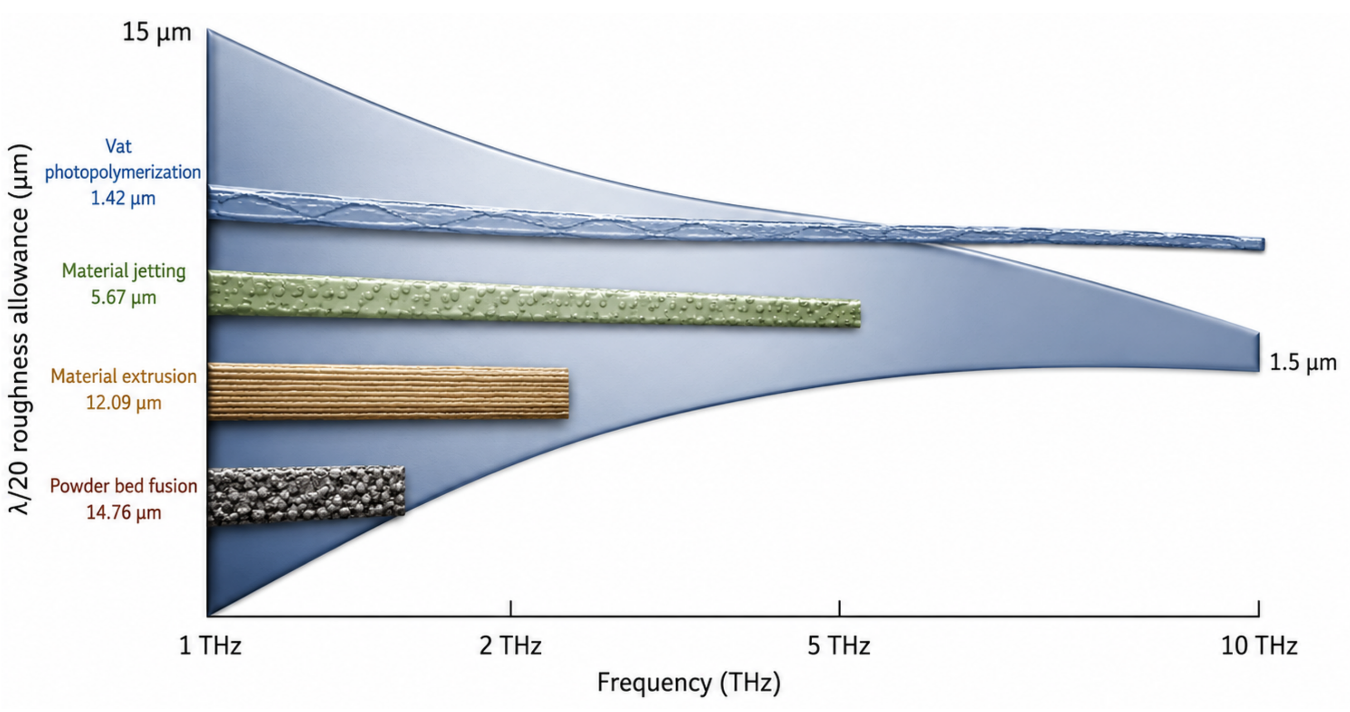

Figure 2: Surface tolerance corridor.

The trend in Figure 2 splits the processes into surface-viable and non-viable groups. The vat photopolymerization with 1.42 μm mean roughness stays inside the corridor in the wide range of frequency. The material jetting at 5.67 μm is placed between high-frequency surface viability and low-frequency applicability. Material extrusion and powder bed fusion exit the high-quality roughness corridor near the low-frequency side and thus require the use of smooth top surface orientation, polishing or coating, or alternatively choosing a lower target frequency for high-quality phase-sensitive optics.

The process entries in Table 2 represent the manufacturing route coordinates. The selection includes powder bed fusion even though the refractive index range and absorption coefficient are unknown for transmissive component scoring, because feature size, roughness and build rate still matter for reflective or structural terahertz component design.

Table 2: Process inputs at 1 THz.

Process	Δn at 1 THz	Lowest α at 1 THz (cm^{-1})	Mean feature size (μm)	Mean roughness (μm)	Mean build rate ($cm^3\ h^{-1}$)
Material extrusion	0.31	1	415.17	12.09	28.74
Material jetting	0.03	24	182.42	5.67	87.45
Vat photopolymerization	0.11	19	80.75	1.42	24.03
Powder bed fusion	N/A	N/A	270.67	14.76	29.82

The values in Table 2 show the two competing advantages. Material extrusion has the best low-loss material and the widest refractive index range, but also the largest feature size. Vat photopolymerization has the best mean roughness and smallest feature size, but its lowest absorption coefficient is high. Material jetting has the highest build rate. Powder bed fusion operates in the vicinity of 1 THz geometry boundary and lacks the necessary dielectric properties for thick transmissive optics.

The process cards in Figure 3 contain the same information in the graphic format and serve as a compact illustration of Table 2. The material textures in the lower part of each card help remember the fact that the numerical values correspond to different physical deposition routes and not to generic printers.

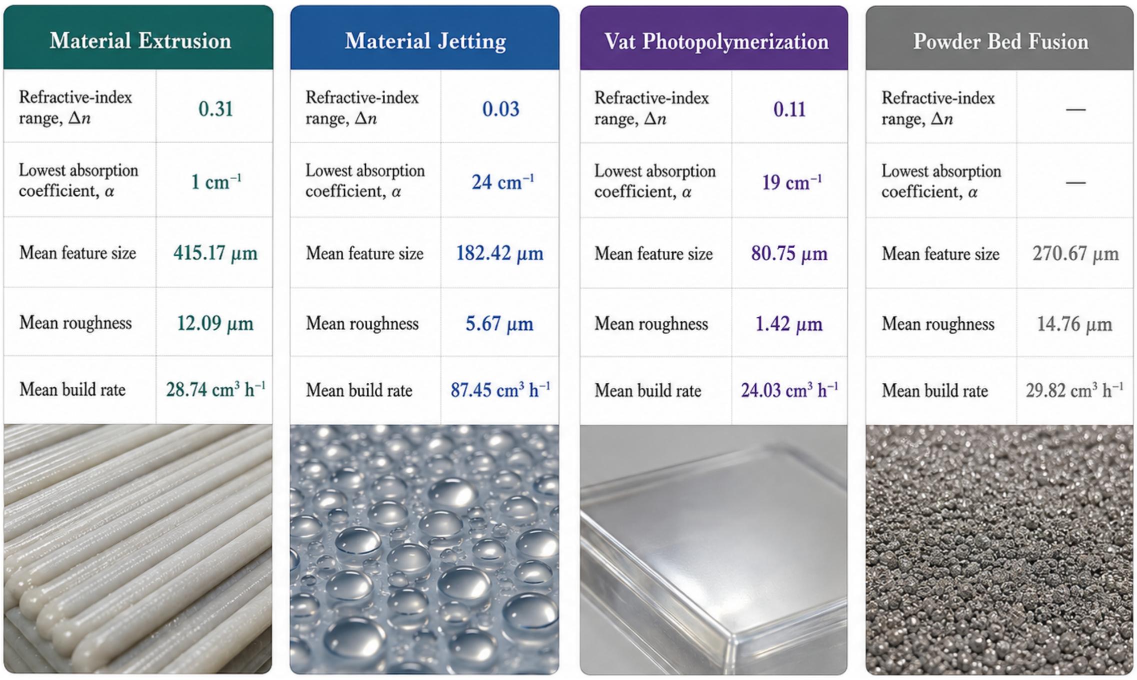

Figure 3: Process inputs.

The most notable trend in Figure 3 is the crossover between geometry and loss. Material extrusion wins in absorption, but loses in feature size. The vat photopolymerization reverses the trend. The material jetting is defined by build rate, but not by transmission. The visual crossover encourages considering the optical thickness in the method section, because a highly absorbing process may be acceptable, provided the optical thickness is small.

Material-level entries in Table 3 demonstrate the reason why the process families should not be considered chemically uniform. Low-loss and high-loss materials coexist within the filament group, and photopolymer entries are mainly in the high-absorption side. These selected optical constants will be used in the following material inventory and transmission interpretation.

The optical constants in Table 3 explain why the optimal filament route is not simply "material extrusion". COC, HDPE and PS represent the low-loss subset, while PLA, PVA and nylon are unusable for thick transmissive optics despite being common printable filaments. At the same time, Table 3 shows the reason why the photopolymer processes cannot be selected based on smoothness: several resins are suitable for phase-relief optics in terms of index, but absorb too much energy at millimeter-scale path length.

Table 3: Selected optical constants at 1 THz.

Material	Printing group	Refractive index at 1 THz	Absorption coefficient at 1 THz (cm^{-1})
COC (TOPAS)	Filament	1.53	1.00
HDPE	Filament	1.53	1.20
PS	Filament	1.56	3.00
HIPS	Filament	1.49	5.00
PC	Filament	1.64	10.00
ABS	Filament	1.57	16.00
PP	Filament	1.48	18.00
Gray Resin	Photopolymer	1.62	19.00
ABS Tough	Photopolymer	1.66	20.50
HTM140 V2	Photopolymer	1.61	21.00
Phrozen Clear	Photopolymer	1.66	21.10
PET-G	Filament	1.60	23.00
RGD450	Photopolymer, material jetting	1.66	24.00
VeroBlue RGD240	Photopolymer, material jetting	1.69	25.00
Formlabs Clear	Photopolymer	1.635	27.00
PLA	Filament	1.64	27.00
TPU	Filament	1.62	29.30
PVA	Filament	1.79	30.60
Nylon	Filament	1.71	32.00

The loss-index distribution in Figure 4 contains the same data as the material-selection map. The visual proximity of COC, HDPE and PS to the lower absorption region explains the importance of material extrusion route despite its large printed features.

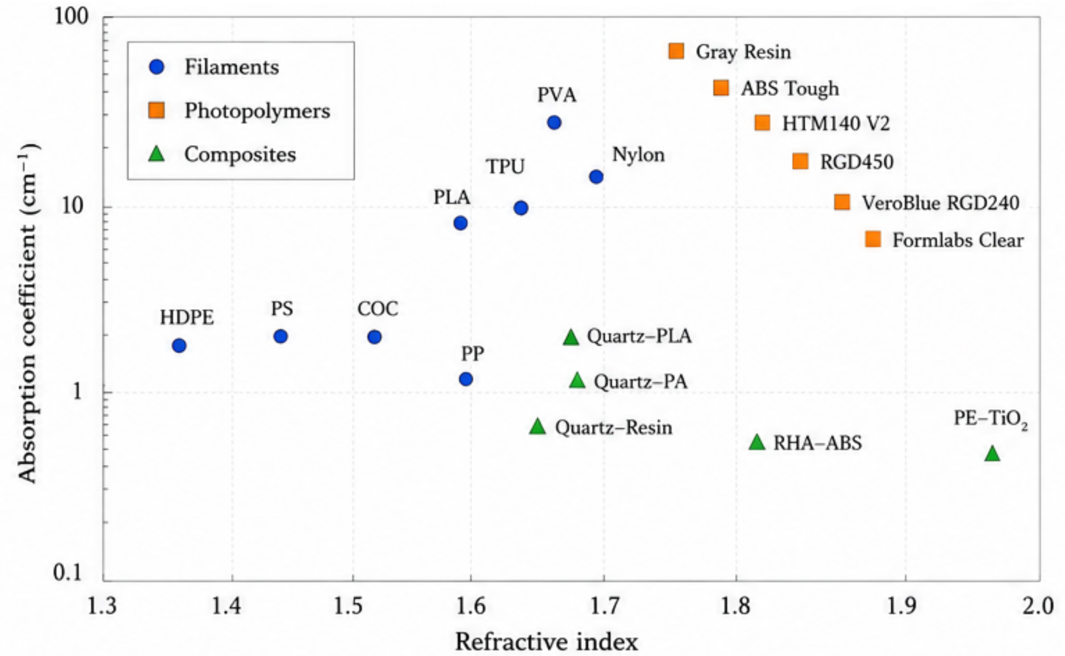

Figure 4: Material loss-index map.

The material inventory in Figure 4 confirms the need to interpret the material rather than process name-based material selection. The low absorption is available in selected non-polar filaments, not in all extruded polymers. Photopolymers are located at higher loss, but their refractive indices are high enough to justify the development of the low-loss resin formula. High-index materials are not necessarily useful if they are accompanied by high absorption.

Composite trajectories expand the material range beyond neat polymers. The quartz-filled thermoplastics illustrate the ability of mineral fillers to shift the terahertz refractive index and absorption simultaneously [47]. The silica-rich rice-husk-ash ABS shows that a sustainable filler material can reduce the loss if dispersed properly [48]. Fully-filled UV resins and $PE\text{-}TiO_2$ systems illustrate that higher index enhancement comes at a greater cost of losses [39]. They are used to check if adding fillers drives the optical properties closer to the optimal terahertz region.

Composites shifts from Figure 5 are considered to outline the direction of material development suggested by process windows. The target in this case is not just maximization of the refractive index, but rather minimization of the absorption, reasonable index value, and printability of the material.

The connected material paths in Figure 5 prove that the direction in addition to the end-point values is important when choosing filler. Filler of quartz or silica family brings a polymer closer to lower absorption level while having modest refractive index increase. It helps when creating transmissive optics. In its turn, TiO_2 brings a material to higher index value but also to higher absorption. This phenomenon can explain why a material having high refractive index fails in being a lens due to lack of compensation of absorption through shortened optical path.

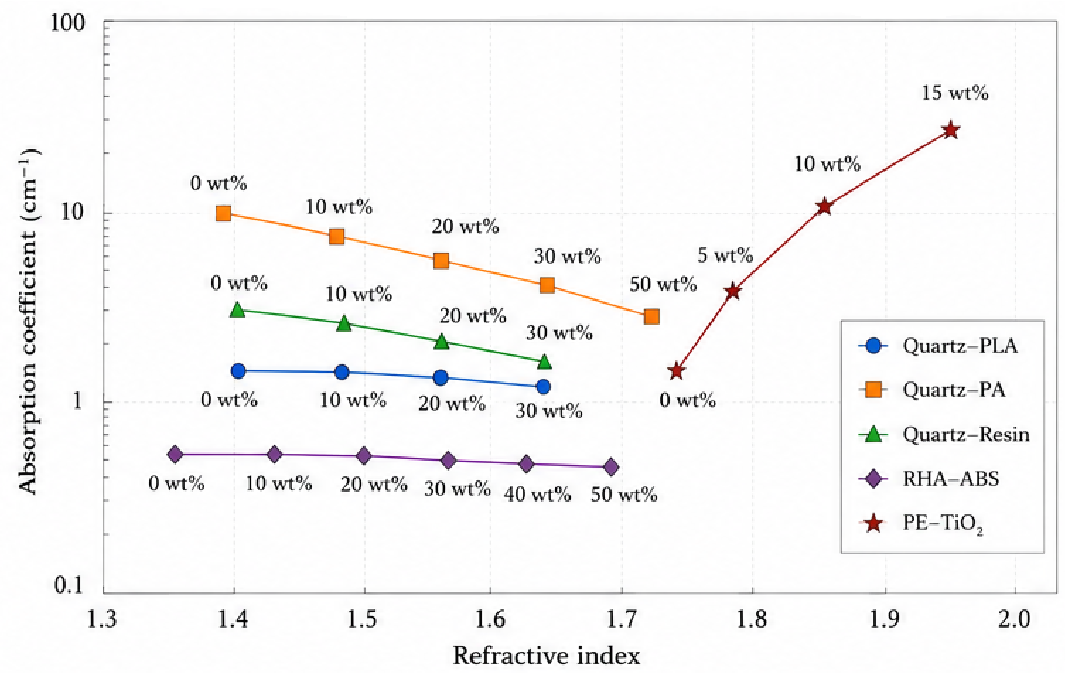

Figure 5: Composite optical shifts.

4. Calculations of Frequency and Thickness

The wavelength in free space at frequency f is calculated as

$$\lambda(f) = \frac{300}{f}. \tag{1}$$

Here, f is measured in THz and λ is measured in micrometres. The feature compatibility ratio of process p is calculated as

$$C_{F,p}(f) = \frac{\lambda(f)}{F_p}, \tag{2}$$

where F_p is the mean minimum feature size. When $C_F \geq 1$ then the mean feature size does not exceed the free-space wavelength. This is a requirement at wavelength scale rather than metamaterial-specific one. Finer diffractive or sub-wavelength structures require greater margin.

The surface compatibility is calculated as

$$C_{R,p}(f) = \frac{\lambda(f)/20}{R_p}, \tag{3}$$

where R_p is the mean process roughness. When $C_R \geq 1$ the surface satisfies high-quality $\lambda/20$ criteria. This formula allows direct conversion of roughness from a static characteristic of the process into an optical constraint depending on frequency.

Geometric ceiling is calculated as

$$f_{G,p} = \min\left(\frac{300}{F_p}, \frac{15}{R_p}\right). \tag{4}$$

This ceiling cannot be treated as universal rejection criteria of the process. It only shows the frequency at which the process requires a smoother surface, smaller feature size, easier optics design or another manufacturing process.

Absorption-limited transmission of the material layer is calculated by

$$T_p(L) = \exp(-\alpha_p L), \tag{5}$$

where α_p is the absorption coefficient in cm^{-1} and L is the optical path length in centimetres. The chosen thickness values are 0.5, 1.0 and 2.0 mm which correspond to $L = 0.05$, 0.10 and 0.20 cm. These represent a thin phase element, compact refractive element and thick lens body.

The route classification is based on Eqs. (2)–(5). A process is said to be geometry-admissible at frequency f when both C_F and C_R are at least unity. A process is said to be transmission-favorable for thickness L when the calculated T remains high compared to other materials. Classification is based on dominant physical limitation rather than a numeric ranking. A process may be acceptable for a thin surface relief part, but unacceptable for a thick lens, even though the same features and roughness parameters apply.

5. Results

The geometry ceiling results in Table 4 identify the maximum frequency where each route meets the wavelength-scale feature condition and $\lambda/20$ roughness condition using the process means. Material extrusion is feature-limited at 0.72 THz. Material jetting is feature-limited at 1.64 THz. Vat photopolymerization is feature-limited at 3.72 THz but remains roughness-compatible up to 10.56 THz. Powder bed fusion is roughness-limited at 1.02 THz and feature-limited at 1.11 THz.

Table 4: Geometry ceilings.

Process	Feature ceiling (THz)	Roughness ceiling (THz)	Governing ceiling (THz)
Material extrusion	0.72	1.24	0.72
Material jetting	1.64	2.65	1.64
Vat photopolymerization	3.72	10.56	3.72
Powder bed fusion	1.11	1.02	1.02

These ceilings define the geometric admissibility boundary. Under the selected wavelength-scale condition, only vat photopolymerization remains geometrically credible at 3 THz among the four common process families. At 1 THz, material jetting, vat photopolymerization and powder bed fusion satisfy the geometry threshold, while material extrusion already falls short in feature size despite having acceptable roughness. This distinction matters because material extrusion may still work for a smooth, weakly featured lens profile, but it should not be treated as geometrically equivalent to a process that can form smaller surface features.

The gauge-style comparison in Figure 6 displays the two ceilings for each route. The lower ceiling governs the allowable operating range and shows whether the limiting geometry is surface roughness or feature size.

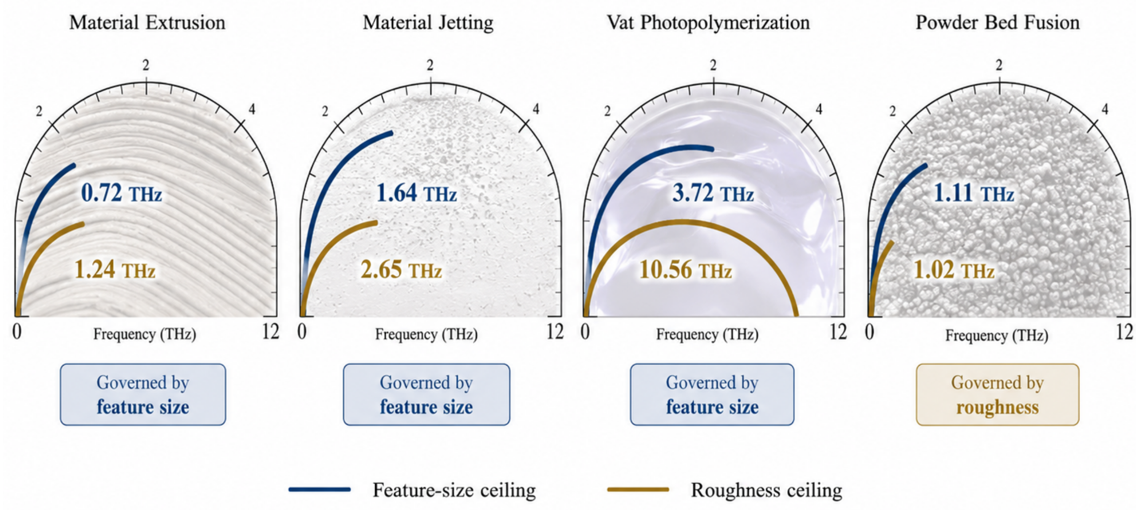

Figure 6: Feature and roughness ceilings.

The ceiling comparison in Figure 6 highlights that roughness is not always the first geometric failure. Material extrusion, material jetting and vat photopolymerization are all limited by feature size in this calculation. Powder bed fusion differs because its roughness ceiling is slightly lower than its feature ceiling, reflecting the granular or partially fused surface character of powder-based parts. The result also shows that vat photopolymerization has a large unused roughness margin relative to its feature ceiling, which means that further process benefit would come from lower-loss resin chemistry or smaller repeatable features, not simply a smoother surface.

The geometry ratios in Table 5 show how process suitability changes at 1, 2 and 3 THz. Values greater than unity satisfy the relevant condition. Material extrusion satisfies roughness but not feature size at 1 THz, and falls below both thresholds at 2 THz. Material jetting satisfies both conditions at 1 THz, only roughness at 2 THz, and neither condition fully at 3 THz.

Vat photopolymerization satisfies both conditions at all three frequencies. Powder bed fusion satisfies both at 1 THz only marginally and then fails both at 2 and 3 THz.

Table 5: Geometry ratios at selected frequencies.

Process	C_F at 1 THz	C_R at 1 THz	C_F at 2 THz	C_R at 2 THz	C_F at 3 THz	C_R at 3 THz
Material extrusion	0.72	1.24	0.36	0.62	0.24	0.41
Material jetting	1.64	2.65	0.82	1.32	0.55	0.88
Vat photopolymerization	3.72	10.56	1.86	5.28	1.24	3.52
Powder bed fusion	1.11	1.02	0.55	0.51	0.37	0.34

The ratio values give a more nuanced interpretation than the ceiling alone. A route slightly below unity may still be usable for a tolerant refractive component, whereas values far below unity indicate severe geometric mismatch. Material extrusion at 1 THz has $C_F = 0.72$, which is a moderate feature deficit for a slowly varying lens but a serious limitation for fine relief. At 3 THz, $C_F = 0.24$ and $C_R = 0.41$, so the same route is no longer credible for phase-sensitive surface control without major process improvement.

Table 6: Path-length transmission.

Process	α (cm^{-1})	T at 0.5 mm	T at 1.0 mm	T at 2.0 mm
Material extrusion	1	0.951	0.905	0.819
Material jetting	24	0.301	0.091	0.008
Vat photopolymerization	19	0.387	0.150	0.022
Powder bed fusion	N/A	N/A	N/A	N/A

Path-length transmission in Table 6 changes the ranking. The absorption-limited transmission of material extrusion is 0.951 at 0.5 mm, 0.905 at 1.0 mm and 0.819 at 2.0 mm when the lowest process-level absorption coefficient of 1 cm^{-1} is used. Vat photopolymerization gives 0.387, 0.150 and 0.022 over the same path lengths. Material jetting gives 0.301, 0.091 and 0.008. Powder bed fusion is not assigned a transmission value because the process-level dielectric constants are unavailable for this transmissive calculation.

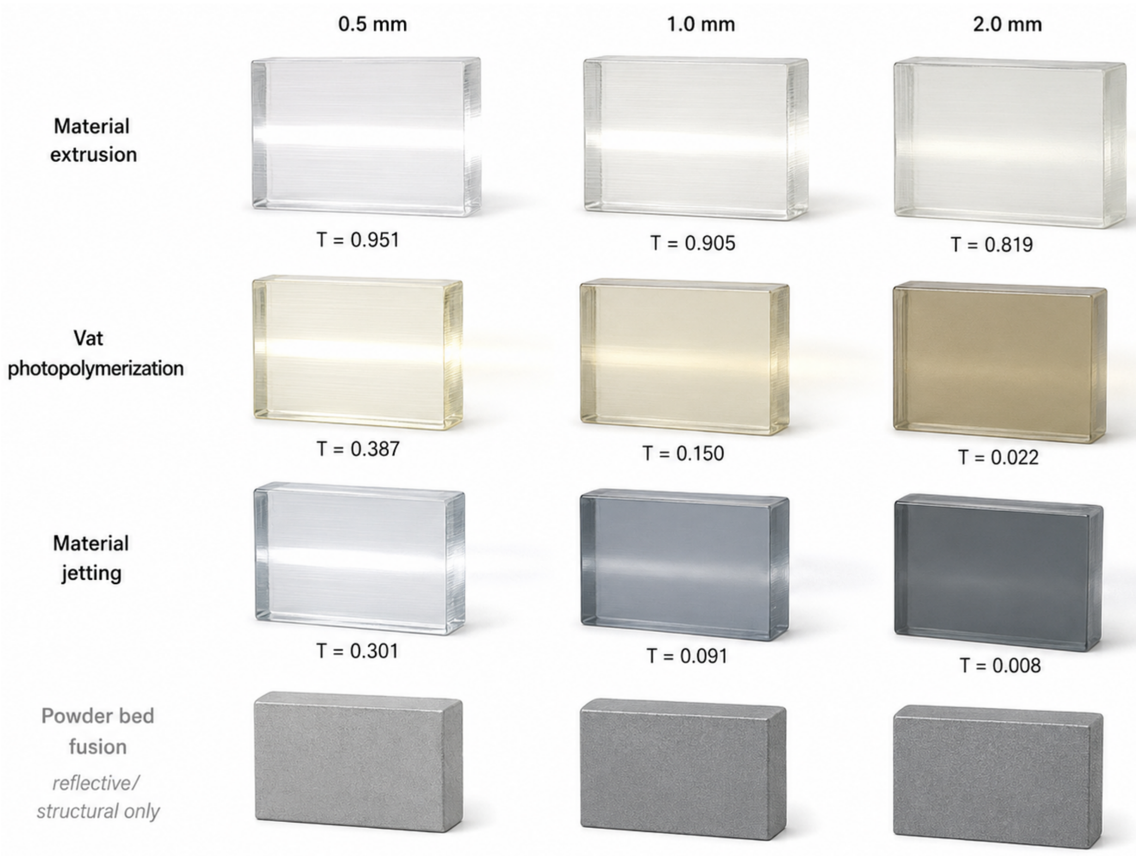

Figure 7: Transmission through printed media.

These transmission values define the optical-thickness boundary. Material extrusion becomes the preferred route for thick low-frequency transmissive optics when a low-loss filament can be printed with sufficient surface quality. Vat photopolymerization can be geometrically superior but loses most intensity at millimetre path lengths if the resin has $\alpha = 19$ cm^{-1}. Material jetting is even more strongly limited by resin loss. The difference between 0.5 and 2.0 mm is decisive: an absorptive photopolymer that may be acceptable as a thin phase plate becomes impractical as a thick lens body.

The material slabs in Figure 7 visualize the same path-length dependence. Bright transmitted bands are retained for low-loss material extrusion, while the photopolymer and material-jetting rows darken rapidly as path length increases.

The optical-thickness contrast in Figure 7 explains why the component type must be named before process selection. A thin phase element can exploit vat photopolymerization geometry if it keeps the material path short. A thick refractive lens cannot ignore absorption simply because the printed surface is smooth. Powder bed fusion is correctly separated from the transmissive rows because its most defensible role is reflective or structural unless low-loss dielectric powder data become available.

The COC parameter response in Figure 8 shows that process settings can shift optical constants rather than only surface geometry. The comparison uses the reported change from an unoptimized condition to a smaller-nozzle optimized condition, where absorption falls from about 10 to 0.7 cm^{-1} and refractive index rises from 1.42 to 1.51.

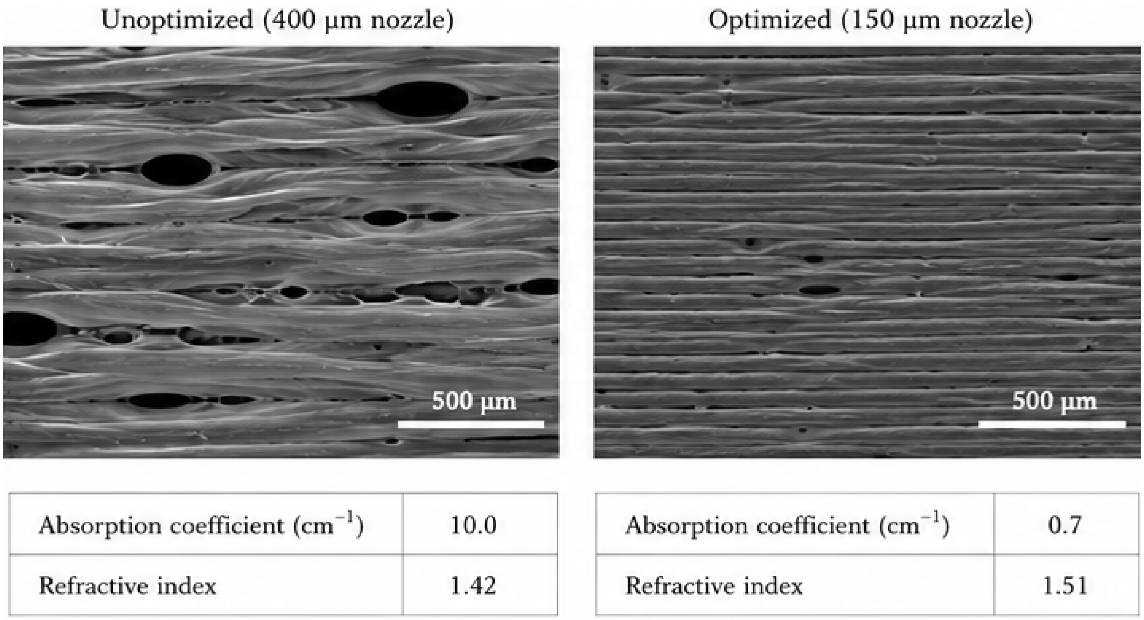

Figure 8: COC printing response.

The microstructural contrast in Figure 8 is important for interpreting material extrusion. The low-loss route depends not only on selecting COC, HDPE or PS, but also on printing those polymers in a dense, uniform and low-void state. A filament that is transparent in bulk can underperform if the printed road structure contains large pores or poor inter-road contact. Conversely, optimized extrusion can move a material into a much stronger transmission window without changing polymer identity.

The component-level assignment in Table 7 combines frequency, path length and component function. It states the manufacturing route implied by the calculated limitations for each component class.

Table 7: Component-level process windows.

Component class	Dominant requirement	Preferred route	Controlling caution
Thick 1 THz refractive lens	High transmission through 1–2 mm	Material extrusion with COC, HDPE or PS	Feature size and surface finish must be controlled
Thin 2–3 THz phase element	Fine geometry and short path	Vat photopolymerization	Resin absorption limits thickness
Short-path repeated array	Throughput and moderate surface fidelity	Material jetting	Path length must remain small
Reflective or structural body	Form, stiffness and post-finishable surface	Powder bed fusion	Surface scattering requires finishing or coating
High-index composite lens	Increased refraction with controlled loss	Silica-rich or quartz-filled printable feedstock	Filler absorption and scattering must remain low

The assignments in Table 7 provide direct design consequences. A thick 1 THz lens should not automatically use the smoothest process; it should prioritize low absorption and then manage the extrusion surface. A 2–3 THz thin phase element should not automatically use the lowest-loss polymer; it should prioritize geometry and restrict path length. A high-throughput array has a different optimum again because build rate matters once the path is short. A metal or powder-bed body must be judged through reflective surface preparation rather than transmissive polymer constants.

The component allocation in Figure 9 converts the table into a compact design map. Each component silhouette is paired with the process family that best matches the calculated limiting condition.

The allocation map in Figure 9 converts the numerical boundaries into a component-specific selection guide. The preferred additive route is the process whose limiting condition is least damaging for the specified component. Low-frequency thick lenses tolerate coarser geometry better than high absorption, while high-frequency thin phase elements tolerate a lossy material only if the path length is short. Reflective bodies move outside the transmissive polymer logic and require surface finishing.

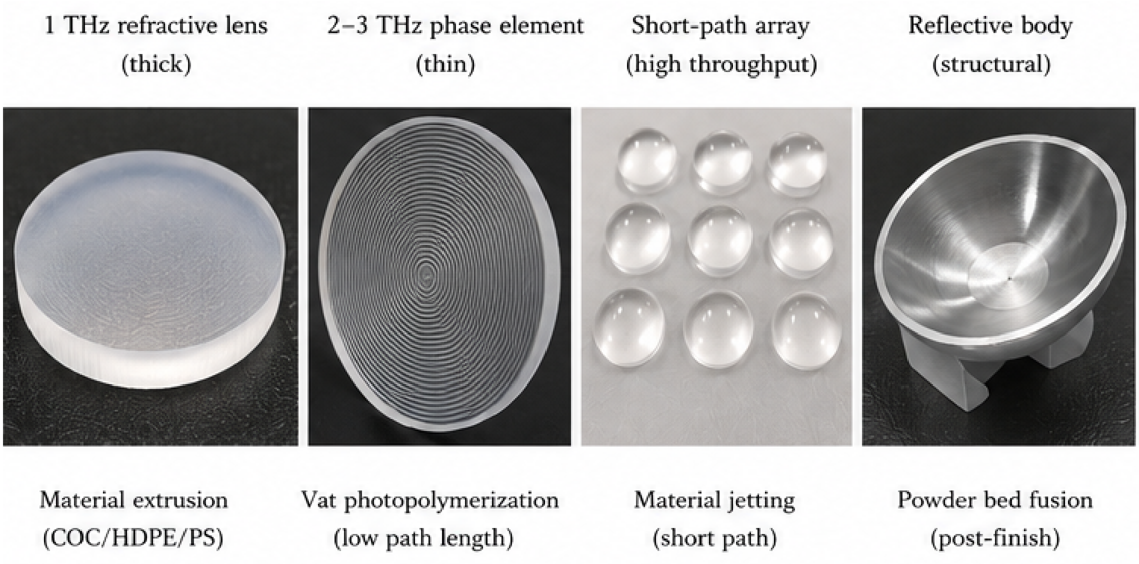

Figure 9: Component-to-process allocation.

6. Discussion

The thickness-frequency calculation provides a new way to think about additive manufacturing for terahertz optics. An average process score conceals the reason why a certain process works or fails. In the current framework, the dominating exclusion is identified: material extrusion is geometry-limited, vat photopolymerization is loss-limited, material jetting is loss- and thickness-limited, and powder bed fusion is transmissive-data-limited for dielectric optics. This classification is important for design because every failure implies a specific solution: geometry limitation can be dealt with via smaller nozzles, finer layer height, optical-face orientation, post-processing or simpler geometry of a component. Loss limitation needs another material chemistry, shorter path length or a switch from refractive to surface-relief components. Transmissive data can be missing because the measurement of dielectric constants for an actual printed state is necessary.

In the case of 1 THz thick lenses, the results support low-loss material extrusion despite the fact that its feature ceiling is below 1 THz. The paradox is explained by component geometry. The smooth refractive lens does not have to cover all its surface with sub-wavelength relief; it needs a precise curvature and good surface finish. COC and HDPE can retain most of the incident energy during millimeter-long paths, and their low loss is more important than geometry precision of a lossy resin. The key is reduction of voids and surface ridges. COC improvement from 10 to 0.7 cm^{-1} after optimization of nozzle and temperature proves that process control has primary importance because it changes the optical state of a material [30]. In the case of extrusion, the most informative validation would be a comparative test of printed density, road bonding, surface roughness and THz transmission for candidate low-loss filaments.

Vat photopolymerization is clearly dominant in geometry for 2–3 THz phase-sensitive optics. The feature ceiling of 3.72 THz and roughness ceiling of 10.56 THz leave it far ahead of material extrusion and material jetting for wavelength-scale surface control. The problem is that a resin with 19 cm^{-1} absorption transmits only 15.0% and 2.2% of incident light through 1 mm and 2 mm, respectively. Consequently, a phase plate produced via vat photopolymerization must be kept thin, be hollowed where possible, or be manufactured using a resin with lower terahertz loss than typical photopolymers. In this context, low-loss photopolymer composites become important while further improvements of stereolithography surface quality become unimportant.

Material jetting is the best choice for short-path or production-oriented devices. The process mean of 87.45 $cm^3\ h^{-1}$ is the largest among four processes, but process-level absorption is the smallest: 24 cm^{-1}. A 1 mm path transmits 9.1% of the light using the simplest calculation. This does not make material jetting useless. It means that the process can be used where the optical path is short, where many similar parts can be printed simultaneously, or where a printed part serves as a thin surface element or alignment component. Reduction of absorption below 5 cm^{-1} by future resins would dramatically improve the competitiveness of this process due to its already good surface quality and throughput.

Powder bed fusion requires another set of evaluation criteria. This process operates near the 1 THz geometrical boundary, but lack of process-level transmissive optical constants precludes a lens-like scoring. For metallic parts, the transmittance is not the goal; reflection, scattering and surface polishing and coating properties are the parameters of interest. Additively manufactured metal reflectors can allow rapid prototyping of terahertz optics, but roughness of as-built surfaces should be reduced for specular performance [15]. Polymer powder bed parts can be difficult to transmit due to high absorption of nylon, but still they could be used as structural mounts and absorbers. In this case, the criteria for evaluation are different from extrusion and photopolymerization. Reflection and polished form accuracy should be considered.

Composite materials represent one of the ways to expand process windows, but the results do not recommend a straightforward strategy of high index. The higher refractive index allows reduction of lens thickness for the same optical power; however, if the filler increases absorption faster than the thickness is reduced, the component becomes worse. The PE–TiO_2 trend represents such situation: the refractive index is significantly increased, but absorption is increased as well. Quartz-filled and silica-rich polymers are more appropriate materials because they could decrease absorption without significant influence on index. The reduction of absorption in rice-husk-ash ABS in comparison with neat ABS shows the possibility of silica-based sustainable fillers with optical value if the particle size, dispersion and scattering are controlled [48]. The ideal material for additive manufacturing of terahertz optics should combine the absorption in COC/HDPE range and surface quality of vat photopolymerization.

This calculation gives insight in usage of the figures and tables of the paper for the purposes of the design. Wavelength and roughness values in Table 1 should be checked prior to the process selection because they determine whether the component is designed in the permissive or restricted frequency band. Process entries in Table 2 inform whether the process should be selected for low-loss polymer optics or it is better to check another one for a different purpose. Material constants in Table 3 prevent wrong generalization based on a process name. Geometrical ceilings in Table 4 tell where the process starts being risky. Transmission values in Table 6 help to estimate whether a printed material survives the planned optical thickness. Finally, the component-window assignments in Table 7 translate the calculations into practical manufacturing choices.

One of the limitations of the calculation is that the inputs represent process means and representative material constants at 1 THz. The real parts could differ from printer model, layer height, orientation, exposure dose, post-curing, infill, filler dispersion and surface finishing. The analysis also uses simple exponential description of absorption, ignores Fresnel reflection, multiple internal reflections, scattering from pores, birefringence, surface-form errors and broadband dispersion. These simplifications are justified during preliminary selection of the process because they allow to save dominant trade-offs without full EM model. Component design should include frequency-dependent index, measured surface form, simulated phase error and experimental transmission of the printed part.

The key result of the calculation is the process switch boundary. If the component is thick and operates near 1 THz, the path-length penalty dominates, and low-loss extrusion is the best route. If the component is thin and operates above 1 THz, the geometry penalty dominates, and vat photopolymerization gets stronger. If the throughput is a key issue and the component is thin, material jetting becomes possible. If the component is reflective or structural, powder bed fusion is to be analyzed using another route. This boundary gives more useful guidance than the universal ranking of additive manufacturing technologies.

7. Conclusion

For a terahertz component designed according to a particular operating frequency and optical thickness, process feasibility is governed by the switching point of absorption against geometry. A thick transmissive element at approximately 1 THz would benefit from material extrusion in order to reduce loss, especially if COC, HDPE, or PS can be extruded with sufficient control of the surface. In the case of $\alpha = 1$ cm^{-1}, the transmission at 1 mm would be 0.905, which is significantly larger than 0.150 obtained for vat photopolymerization and 0.091 for material jetting, with the same path length. Therefore, material extrusion does not become infeasible for making lenses due to the 0.72 THz feature limit, but only due to the requirements of the optical geometry.

The situation is different for higher frequencies or phase-sensitive optics. In such cases, vat photopolymerization would be the most feasible common process for 2–3 THz thin optics because it maintains the ratio of feature size and roughness versus wavelength larger than 1 up to 3 THz. Thus, its limitation would be absorption rather than geometry. It is concluded that vat photopolymerization is the process to use for thin surface-relief elements, hollowed optics, and short path length components unless a low-absorption resin chemistry is available. Material jetting is suitable for short-path arrays and throughput-demanding parts, while powder bed fusion is meant for reflective or structural terahertz optics in which surface finish and coatings define the optical properties rather than dielectric transmission.

The selection rule is conditional: the chosen process is the one with a limiting condition least harmful for the particular frequency-thickness pair. Thus, a 1 THz thick lens should favor low loss and tolerate the extrusion geometry. A 2–3 THz thin phase element should favor fine geometry and impose the photopolymer path length limitation. Reflective body should favor post-finished surface rather than dielectric transmission. The future development should rely on finding low-loss or non-polar materials or silica-rich ones with high-resolution photopolymerization, and on measuring optical constants of printed parts.

Conflict of Interest

The author declares no conflict of interest.

References

[1] Tonouchi, M. (2007). Cutting-edge terahertz technology. Nature photonics, 1(2), 97-105.
[2] Lee, Y. S. (2009). Principles of terahertz science and technology (Vol. 170). Springer Science & Business Media.
[3] Zhang, X. C., & Xu, J. (2010). Introduction to THz wave photonics (Vol. 29, p. 246). New York: Springer.
[4] Mittleman, D. M. (2017). Perspective: Terahertz science and technology. Journal of Applied Physics, 122(23).
[5] Akyildiz, I. F., Jornet, J. M., & Han, C. (2014). Terahertz band: Next frontier for wireless communications. Physical communication, 12, 16-32.
[6] Ferguson, B., & Zhang, X. C. (2002). Materials for terahertz science and technology. Nature materials, 1(1), 26-33.
[7] Jepsen, P. U., Cooke, D. G., & Koch, M. (2011). Terahertz spectroscopy and imaging–Modern techniques and applications. Laser & Photonics Reviews, 5(1), 124-166.
[8] Siemion, A. (2020). The magic of optics—an overview of recent advanced terahertz diffractive optical elements. Sensors, 21(1), 100.
[9] Kaur, A., Myers, J. C., Ghazali, M. I. M., Byford, J., & Chahal, P. (2015, May). Affordable terahertz components using 3D printing. In 2015 IEEE 65th Electronic Components and Technology Conference (ECTC) (pp. 2071-2076). IEEE.
[10] Squires, A. D., Constable, E., & Lewis, R. A. (2015). 3D printed terahertz diffraction gratings and lenses. Journal of infrared, millimeter, and terahertz waves, 36(1), 72-80.
[11] Furlan, W. D., Ferrando, V., Monsoriu, J. A., Zagrajek, P., Czerwińska, E., & Szustakowski, M. (2016). 3D printed diffractive terahertz lenses. Optics letters, 41(8), 1748-1751.
[12] Liu, C., Liu, J., Niu, L., Wei, X., Wang, K., & Yang, Z. (2017). Terahertz circular Airy vortex beams. Scientific reports, 7(1), 3891.
[13] Yang, S., Sheng, X., Zhao, G., Lou, S., & Guo, J. (2021). 3D printed effective single-mode terahertz antiresonant hollow core fiber. IEEE Access, 9, 29599-29608.
[14] Rohrbach, D., Kang, B. J., & Feurer, T. (2021). 3D-printed THz wave-and phaseplates. Optics express, 29(17), 27160-27170.
[15] Headland, D., Withayachumnankul, W., Webb, M., Ebendorff-Heidepriem, H., Luiten, A., & Abbott, D. (2016). Analysis of 3D-printed metal for rapid-prototyped reflective terahertz optics. Optics express, 24(15), 17384-17396.
[16] Zhu, Y., Tang, T., Zhao, S., Joralmon, D., Poit, Z., Ahire, B., ... & Li, X. (2022). Recent advancements and applications in 3D printing of functional optics. Additive Manufacturing, 52, 102682.
[17] Blachowicz, T., Ehrmann, G., & Ehrmann, A. (2021). Optical elements from 3D printed polymers. e-Polymers, 21(1), 549-565.
[18] Busch, S. F., Weidenbach, M., Fey, M., Schäfer, F., Probst, T., & Koch, M. (2014). Optical properties of 3D printable plastics in the THz regime and their application for 3D printed THz optics. Journal of Infrared, Millimeter, and Terahertz Waves, 35(12), 993-997.
[19] Squires, A. D., & Lewis, R. A. (2018). Feasibility and characterization of common and exotic filaments for use in 3D printed terahertz devices. Journal of Infrared, Millimeter, and Terahertz Waves, 39(7), 614-635.
[20] Brodie, C. H., Spotts, I., Reguigui, H., Leclerc, C. A., Mitchell, M. E., Holzman, J. F., & Collier, C. M. (2022). Comprehensive study of 3D printing materials over the terahertz regime: absorption coefficient and refractive index characterizations. Optical Materials Express, 12(9), 3379-3402.
[21] Duangrit, N., Hong, B., Burnett, A. D., Akkaraekthalin, P., Robertson, I. D., & Somjit, N. (2019). Terahertz dielectric property characterization of photopolymers for additive manufacturing. IEEE Access, 7, 12339-12347.
[22] Castro-Camus, E., Koch, M., & Hernandez-Serrano, A. I. (2020). Additive manufacture of photonic components for the terahertz band. Journal of Applied Physics, 127(21).
[23] Golhin, A. P., Tonello, R., Frisvad, J. R., Grammatikos, S., & Strandlie, A. (2023). Surface roughness of as-printed polymers: a comprehensive review. The International Journal of Advanced Manufacturing Technology, 127(3), 987-1043.
[24] Neu, J., & Schmuttenmaer, C. A. (2018). Tutorial: An introduction to terahertz time domain spectroscopy (THz-TDS). Journal of Applied Physics, 124(23).
[25] Liebermeister, L., Nellen, S., Kohlhaas, R. B., Lauck, S., Deumer, M., Breuer, S., ... & Globisch, B. (2021). Terahertz multilayer thickness measurements: Comparison of optoelectronic time and frequency domain systems. Journal of Infrared, Millimeter, and Terahertz Waves, 42(11), 1153-1167.
[26] Cunningham, P. D., Valdes, N. N., Vallejo, F. A., Hayden, L. M., Polishak, B., Zhou, X. H., ... & Twieg, R. J. (2011). Broadband terahertz characterization of the refractive index and absorption of some important polymeric and organic electro-optic materials. Journal of applied physics, 109(4), 043505-043505.
[27] Wietzke, S., Jansen, C., Reuter, M., Jung, T., Kraft, D., Chatterjee, S., ... & Koch, M. (2011). Terahertz spectroscopy on polymers: A review of morphological studies. Journal of Molecular Structure, 1006(1-3), 41-51.
[28] D'Angelo, F., Mics, Z., Bonn, M., & Turchinovich, D. (2014). Ultra-broadband THz time-domain spectroscopy of common polymers using THz air photonics. Optics express, 22(10), 12475-12485.
[29] Xiao, H., Huang, J., Wang, M., Huang, W., Li, M., & Jin, G. (2024). Unraveling molecular loss processes for dielectric polymers in the Terahertz frequency range: Impact of polarity and chain rigidity. Polymer, 297, 126855.
[30] Mavrona, E., Graf, J., Hack, E., & Zolliker, P. (2020, November). Towards high quality 3D printed THz devices with cyclic olefin polymer. In 2020 45th International Conference on Infrared, Millimeter, and Terahertz Waves (IRMMW-THz) (pp. 1-2). IEEE.
[31] Clark, A. T., Federici, J. F., & Gatley, I. (2021). Effect of 3D printing parameters on the refractive index, attenuation coefficient, and birefringence of plastics in terahertz range. Advances in Materials Science and Engineering, 2021(1), 8276378.
[32] Naftaly, M., Savvides, G., Alshareef, F., Flanigan, P., Lui, G., Florescu, M., & Mullen, R. A. (2022). Non-destructive porosity measurements of 3D printed polymer by terahertz time-domain spectroscopy. Applied Sciences, 12(2), 927.
[33] Kaluza, M., Walczakowski, M., & Siemion, A. (2024). Exploring the impact of 3D printing parameters on the THz optical characteristics of COC material. Materials, 17(20), 5104.
[34] Macdonald, N. P., Cabot, J. M., Smejkal, P., Guijt, R. M., Paull, B., & Breadmore, M. C. (2017). Comparing microfluidic performance of three-dimensional (3D) printing platforms. Analytical chemistry, 89(7), 3858-3866.
[35] Bhushan, B., & Caspers, M. (2017). An overview of additive manufacturing (3D printing) for microfabrication. Microsystem Technologies, 23(4), 1117-1124.

[36] Zhang, B., Guo, Y. X., Zirath, H., & Zhang, Y. P. (2017). Investigation on 3-D-printing technologies for millimeter-wave and terahertz applications. Proceedings of the IEEE, 105(4), 723-736.

[37] Malas, A., Isakov, D., Couling, K., & Gibbons, G. J. (2019). Fabrication of high permittivity resin composite for vat photopolymerization 3D printing: Morphology, thermal, dynamic mechanical and dielectric properties. Materials, 12(23), 3818.

[38] Shah, D. M., Morris, J., Plaisted, T. A., Amirkhizi, A. V., & Hansen, C. J. (2021). Highly filled resins for DLP-based printing of low density, high modulus materials. Additive Manufacturing, 37, 101736.

[39] Peng, H. Y., Wei, Y. A., Hsu, Y. C., Lin, K. C., Yeh, P. Y., Yang, C. S., & Cheng, C. P. (2021). Complex optical properties of polymeric composite materials mixed with quartz powder and investigated by THz time-domain spectroscopy. Optical Materials Express, 12(1), 22-33.

[40] Yu, Y., Zhang, Z., Zhang, T., Zhao, X., Chen, Y., Cao, C., ... & Xu, K. (2020). Effects of surface roughness on terahertz transmission spectra. Optical & Quantum Electronics, 52(5), 1.

[41] Xie, P., Guan, K., He, D., Yi, H., Dou, J., & Zhong, Z. (2022). Terahertz wave propagation characteristics on rough surfaces based on full-wave simulations. Radio Science, 57(6), 1-16.

[42] Syrlybayev, D., Seisekulova, A., Talamona, D., & Perveen, A. (2022). The post-processing of additive manufactured polymeric and metallic parts. Journal of Manufacturing and Materials Processing, 6(5), 116.

[43] Turek, P., Bazan, A., & Zakrecki, A. (2024). Influence of post-processing treatment on the surface roughness of polyamide PA12 samples manufactured using additive methods in the context of the production of orthoses. Proceedings of the Institution of Mechanical Engineers, Part B: Journal of Engineering Manufacture, 238(11), 1694-1708.

[44] Mao, M., He, J., Li, X., Zhang, B., Lei, Q., Liu, Y., & Li, D. (2017). The emerging frontiers and applications of high-resolution 3D printing. Micromachines, 8(4), 113.

[45] Cai, F., Chang, Y. H., Wang, K., Zhang, C., Wang, B., & Papapolymerou, J. (2016). Low-loss 3-D multilayer transmission lines and interconnects fabricated by additive manufacturing technologies. IEEE Transactions on Microwave Theory and Techniques, 64(10), 3208-3216.

[46] Phillips, L., Valavanis, A., Burnett, A. D., Kay, R., Harris, R., & Saleh, E. (2025). Process and material constraints of additive manufacturing for fabrication of terahertz quasi-optical components. Applied Materials Today, 42, 102619.

[47] Nakanishi, A., & Satozono, H. (2020). Terahertz optical properties of wood–plastic composites. Applied optics, 59(4), 904-909.

[48] Peng, H. Y., Yang, C. S., Wei, Y. A., Ruan, Y. C., Hsu, Y. C., Hsieh, C. F., & Cheng, C. P. (2021). Terahertz complex refractive index properties of acrylonitrile butadiene styrene with rice husk ash and its possible applications in 3D printing techniques. Optical Materials Express, 11(9), 2777-2786.